Stability and excitations of spontaneous vortices in polariton condensates

Ting-Wei Chen [a], Yu-Ling Chiang [b], Szu-Cheng Cheng [b],*, Wen-Feng Hsieh [c],*

[a] Department of Photonics, National Cheng Kung University, Tainan 701, Taiwan
[b] Department of Physics, Chinese Culture University, Taipei 111, Taiwan
[c] Department of Photonics and Institute of Electro-Optical Engineering, National Chiao Tung University, Hsinchu 300, Taiwan

ABSTRACT

We study the dynamics of spontaneously formed vortices in incoherently pumped homogeneous microcavity polariton condensates (MPC). We find vortices are stable and appear spontaneously without stirring or rotating MPCs by the numerical modeling using complex Gross–Pitaevskii equation. The center of the vortex core contains some background of reservoir polaritons and the visibility increases with the pump strength. The vortex radius is inversely proportional to the square root of the condensate density or the pump strength. Finally, vortices formed by low pumping power exhibit short lifetime because of the existence of excitations without costing energy.

© 2013 Elsevier Ltd. All rights reserved.

1. Introduction

Bose–Einstein condensation (BEC) is a macroscopic phenomenon from a quantum state due to the coherence of bosons below the transition temperature [1,2]. The transition temperature of the condensate is inversely proportional to the mass of particles. Excitons coupled to localized photons in a microcavity containing semiconductor quantum wells form microcavity polaritons having 5 orders of magnitude lighter mass than electrons [3]. Because of the ultra-light polariton mass, the transition temperature of microcavity polaritons could be raised up to room temperature [4]. In the past decade, scientists took a lot of efforts to observe microcavity-polariton condensates (MPCs). Growing interest in MPCs can be attributed to the system being intrinsically out-of-equilibrium with the steady state determined by the dynamical balance between interactions, pumping and decay [5–7]. The momentum space distributions of MPCs were measured and the accumulation of polaritons in the lowest energy state (or condensation) was first observed in planar CdTe and GaAs microcavities [2,8]. Deng et al. [1] measured the second-order coherence functions of a MPC and distinguish it from a non-condensate. Due to the continuous pumping and disorders of MPCs, vortices observed in MPCs give the definite evidence of MPC [9]. Spontaneous vortex formation is also one of the major features for the superfluid phase transition. It is surprising that vortices appear spontaneously without stirring or rotating

MPCs [6,7,9,10], however, non-equilibrium MPCs show the instability of forming vortices and spontaneous array of vortices without any rotational drive [6,7,9,10]. Therefore, it is important to understand the vortex structure and its stability through studying the dynamics of MPCs. At this moment, there is still lack of a consistent theory to interpret all the observed properties of vortices in MPCs.

It is also unique that the vortex radius in MPCs is on the order of the healing length and is typically 2 orders of magnitude larger than that in atomic condensates and thus is large enough to be observed directly [11]. The vortex radius is given by the healing length determined by polariton–polariton interactions and is inversely proportional to the square root of the condensate density or lower polariton blueshift [11,12]. The coreless (nonzero density at center) vortex can be observed because it contains some background of polaritons from the reservoir. Two components are added so that the experimental observation is not purely the angular momentum state with quantum number $\ell = 1$. Due to the repulsive interactions of polaritons, the chemical potential of the condensate goes higher and creates a blue shift on the total energy as a high density of polaritons has been injected into the system by raising the pumping power [13]. Spontaneous vortices were experimentally observed in atomic BECs and polariton systems in the presence of external confining or disorder potentials [6,9,14,15]. In the Kibble–Zurek mechanism [16], the excitations of topological defects can be formed when going through the phase transition, and finally get pinned to the disorders. A correlation length ξ and hence the spontaneous topological defect density (proportional to $1/\xi^2$) are determined by the

* Corresponding authors. Tel.: +886 35712121x56316; fax: +885 35716631.
E-mail addresses: sccheng@faculty.pccu.edu.tw (S.-C. Cheng),
wfshieh@mail.nctu.edu.tw (W.-F. Hsieh).

quench rate of the system through the critical temperature. The remarkable observation made is that the phase transition occurs over a finite time, and the system falls out of equilibrium when the thermalization (or relaxation) rate drops below a quench rate $1/\tau_Q$ [15,16]. In this scenerio, vortices are formed during the merging of isolated coherent regions with uncorrelated phases.

In polariton superfluids, the spontaneous vortex generation can be a manifestation of the Kibble–Zurek mechanism. These vortices would migrate and not be visible after averaging over many experiments, but give a decrease of fringe contrast of the interferometric images. A numerical modeling using the sto-chastic Gross–Pitaevskii equation was performed by Lagoudakis et al. [14] to reproduce the preferential vortex paths and explain the experimental observations. Vortices can also be generated using a weak external imprinting laser beam in a coherent optical-parametric-oscillator system [10–12], however, a mini-mum power is required for the polaritons to acquire enough angular momentum to create a vortex. The vortex lifetime is long for high excitation power and vice versa [12], whereas, vortices in incoherently pumped MPCs are stabilized by dis-orders and have negligible dependence on the excitation con-ditions [9].

In this paper, we shall show that even in a system without disorders or confinements, vortices sensitive to the excitation conditions are stable and arise spontaneously due to the driven-dissipative nature. The vortex state of MPCs is studied through the complex Gross–Pitaevskii equation (cGPE) coupled to the reservoir polaritons at high momenta [5]. This mean-field model for non-equilibrium MPCs is a generic model of considering effects from pumping, dissipation, potential trap, relaxation and interactions. In Section 2, without considering a potential trap or disorders, we study the dynamics of spontaneously formed vortices in incoherently pumped MPCs. The steady state of the system with a vortex is analyzed under a uniform pumping power, P. Furthermore, the visibility and core radius of the singly quantized vortex are calculated as a function of pumping power. We find that the size of a vortex is inversely proportional to the square root of the condensate density or the pumping power above the threshold. Moreover, with increasing pumping powers, the core radius and visibility, which are determined by decay rates of the condensate and the reservoir polaritons, of a vortex become smaller and higher, respectively. In Section 3, from the steady state of the system with a specific vorticity, the stability and collective-excitation spectra of a vortex is investigated by utilizing the Bogoliubov theory. Because of the non-equilibrium character of MPCs, the excitation frequency Ω is a complex value [5,17], whose real part, Re(Ω), and imaginary part, Im(Ω), repre-sent excitation energy and decay or growth rate of the system. The stability of the singly quantized vortex is justified by Im(Ω) provided that Im(Ω) < 0. We show that singly quantized vortices can still exist and remain stable under fluctuations even in the absence of stirring, rotating, trapping, or disorders. We shall present the conclusions in Section 4.

2. Dynamics of spontaneously formed vortices

In order to study non-equilibrium MPCs, we treat the polar-itons at high momenta as a reservoir whose state is determined by the reservoir density, $n_R(\mathbf{r},t)$, and employ the cGPE, governing the condensate polaritons that couples to the reservoir polaritons, to describe the time evolution and density distribution of the con-densate. The wave function $\Psi(\mathbf{r},t)$ of the condensate and the reservoir density satisfy the coupled differential equations as

below

$$i\hbar\frac{\partial\Psi}{\partial t} = -\frac{\hbar^2}{2m}\nabla^2\Psi + \frac{i\hbar}{2}[R(n_R)-\gamma]\Psi + g|\Psi|^2\Psi + 2\tilde{g}n_R\Psi \quad (1)$$

$$\frac{\partial n_R}{\partial t} = P - \gamma_R n_R - R(n_R)|\Psi|^2 \quad (2)$$

where γ_R and γ are the decay rates of reservoir and condensate polaritons; g and $\tilde{g}$ are the strength of polariton–polariton inter-actions and the coupling constant between the condensate and reservoir; and $R(n_R)$ is the amplification rate that describes the replenishment of the condensate state from the reservoir state by stimulated scattering. To simplify our calculation, hereafter we assume the condensate is of two dimensional with no radially confined trapping potential. The system is located in the plane perpendicular to the pumping axis, which is also the confinement direction of the excitons in the quantum wells.

In the steady state, the reservoir density is $n_R(\mathbf{r},t)=n_R^0$ and the wave function can be described by $\Psi(\mathbf{r},t)=\Psi_0(\mathbf{r})e^{-i\mu t/\hbar}$ with chemical potential μ and Planck's constant $\hbar$. If the pumping power P is below the threshold P_{th} or $P < P_{th}$, there is no condensate density ($\Psi_0(r)=0$) and the reservoir density is proportional to the pumping power, i.e., $n_R^0=P/\gamma_R$. At the threshold, the reservoir density $n_R^{th}=P_{th}/\gamma_R$ is fixed by the balance between the amplifica-tion rate $R(n_R(\mathbf{r},t))$ and decay rate γ of the condensate, i.e., $R(n_R^{th})=\gamma$. When $P > P_{th}$, a condensate appears and the condensate density, defined as $n_c=|\Psi_0(\mathbf{r})|^2$, far away from the vortex core region grows as $n_c=(P_{th}/\gamma)\alpha$, where $\alpha=(P/P_{th})-1$ is called the pump coefficient being the relative pumping intensity above the threshold. In the mean time, the stationary reservoir density, which is determined by the net gain being zero, is equal to the reservoir density at the threshold pump power, $n_R^0=n_R^{th}$. Then, the chemical potential of the system is $\mu=gn_c+2\tilde{g}n_R^0$. Throughout this paper we shall take $\tilde{g}=2g$ under the Hartree–Fock approximation. Given the length unit $\lambda=\sqrt{\hbar^2\gamma\sigma/2mgP_{th}}$ and energy unit $\hbar\omega_0=\hbar^2/2\,m\lambda^2$, where m is the polariton mass and $\sigma=1/[1-(4\gamma/\gamma_R)]$, we can choose the length, time and energy scales in units of λ, $1/\omega_0$ and $\hbar\omega_0$, respectively. Also rescaling the wave function $\Psi(\mathbf{r},t)\rightarrow\sqrt{n_c}\cdot\psi(\boldsymbol{\rho},t)$ and reservoir density $n_R(\mathbf{r},t)\rightarrow n_R^{th}\cdot n(\boldsymbol{\rho},t)$, where $\boldsymbol{\rho}=(\rho,\theta)$ is the two dimensional polar coordinate system with the dimensionless radial coordinate $\rho=r/\lambda$, the cGPE of $\psi(\boldsymbol{\rho},t)$ and the rate equation of $n(\boldsymbol{\rho},t)$ are given as

$$i\frac{\partial\psi}{\partial\tau} = -\nabla_\rho^2\psi + \frac{i}{2}\left[\tilde{R}(n)-\tilde{\gamma}\right]\psi + \alpha\sigma|\psi|^2\psi + (\sigma-1)n\psi, \quad (3)$$

$$\frac{\partial n}{\partial\tau} = \tilde{\gamma}_R(\alpha+1-n) - \alpha\tilde{R}(n)\frac{\tilde{\gamma}_R}{\tilde{\gamma}}|\psi|^2, \quad (4)$$

where $\tilde{R}(n)=R(n)/\omega_0$, $\tilde{\gamma}=\gamma/\omega_0$, $\tilde{\gamma}_R=\gamma_R/\omega_0$ and

$$\nabla_\rho^2 = \frac{1}{\rho}\frac{\partial}{\partial\rho}\left(\rho\frac{\partial}{\partial\rho}\right) + \frac{1}{\rho^2}\frac{\partial^2}{\partial\theta^2} \quad (5)$$

is the Laplacian operator associated with the dimensionless polar coordinate $\rho=r/\lambda$.

The steady state of the system under a uniform pumping can be obtained by substituting $\psi=\psi_0 e^{-i\tilde{\mu}t}$ and $n(\boldsymbol{\rho},t)=n_0$ into Eqs. (3) and (4), where $\tilde{\mu}=\mu/\hbar\omega_0$ is the dimensionless chemical potential of the system. Using $\tilde{R}(n)=\tilde{\gamma}$ for the stationary condition, we then have the stationary reservoir density $n_0=\alpha+1-\alpha|\psi_0|^2$ from Eq. (4). Therefore, the densities of reservoir polaritons and the condensate are locked together determined by the following time-independent nonlinear Schrödinger equation:

$$-\nabla_\rho^2\psi_0 + \alpha|\psi_0|^2\psi_0 + (\sigma-1)(\alpha+1)\psi_0 = \tilde{\mu}\psi_0. \quad (6)$$

In the region far away from the vortex core, the density of the system is uniform with $\psi_0\rightarrow1$ and $n_0\rightarrow1$. We then find the

chemical potential of the system, $\tilde{\mu} = \alpha\sigma + (\sigma-1)$, from Eq. (6). Substituting $\tilde{\mu}$ back to Eq. (6), we obtain

$$\nabla_\rho^2 \psi_0 + \alpha(1-|\psi_0|^2)\psi_0 = 0, \tag{7}$$

which has been used to describe a vortex profile with healing length $\xi = \lambda/\sqrt{\alpha}$ or $\xi = \sqrt{\hbar^2\gamma\sigma/2mgP_{th}\alpha}$ [10,11]. The healing length of vortices is inversely proportional to the square root of the pumping power that can be understood qualitatively by equating a typical kinetic energy associated with a vortex in the condensate, $\sim(2m\xi^2)^{-1}$, to the blue-shifted interaction energy of $\sim gn$. Thus, the healing length ξ can be represented as $(2mgn)^{-1/2}$ and the condensate density n_c increases with pumping power. The role of pumping power P here can be interpreted in two ways. First, it is in proportion to the vortex density so that the inverse power proportionality to the correlation length ξ (defect density $\sim 1/\xi^2$) can be retrieved. Secondly, the pumping power is in analogy to the quench rate of the entire system. When the pumping power is greater than a threshold power determined by the decay rate of reservoir, i.e., $P_{th} = \gamma_R n_R^{th}$, the sysytems falls out of equilibrium with the additional power used to replenish the condensated polaritons. From this point of view, the pumping power acts like the quench rate in Kibble–Zurek scenerio for the spontaneous vortex generation. From $n_c = (P_{th}/\gamma)\alpha$ far from the vortex core region in our system, we also conclude the healing length of vortices is inversely proportional to the square root of the condensate density far away from the core, i.e., $\xi \propto n_c^{-1/2}$. Therefore the vortex radius (a_V) is also inversely proportional to the square root of the condensate density that is consistent with the experiments [11,12].

To find the steady state of a vortex, we just need to solve Eq. (7) and find ψ_0 for $\alpha=1$, i.e., $\psi_0^{\alpha=1}(\rho,\theta)$, then the solution $\psi_0^\alpha(\rho,\theta)$ for other pump coefficients α can be obtained by rescaling the length scale, i.e., $\psi_0^\alpha(\rho,\theta) = \psi_0^{\alpha=1}(\sqrt{\alpha}\rho,\theta)$. We assume the steady-state solution is $\psi_0(\rho,\theta) = f(\rho)e^{i\ell\theta}$ with ℓ representing the winding number of the quantized vortex. Then Eq. (7) becomes

$$\frac{d^2f}{d\rho^2} + \frac{1}{\rho}\frac{df}{d\rho} - \frac{\ell^2}{\rho^2}f + \alpha(1-f^2)f = 0. \tag{8}$$

$f(\rho)$ is numerically solved for a given pumping power α. Then the total density of the system, $N(\rho)$, is given by $N(\rho) = \chi(\rho) + \kappa(\rho)$, where

$$\chi(\rho) = n_R^{th}(\gamma_R/\gamma)\alpha f^2(\rho) \tag{9}$$

and

$$\kappa(\rho) = n_R^{th}[\alpha + 1 - \alpha f^2(\rho)] \tag{10}$$

are the density profiles of the condensate and reservoir polaritons, respectively. We then conclude that the vortex core structure is a combination of the condensate and reservoir polaritons. Due to the density of reservoir polaritons at $\rho=0$ being not zero and equal to $\kappa(\rho=0) = n_R^{th}(\alpha+1)$, the total density of the system is not zero at the center of the vortex. Therefore, the dip in the vortex core contains some background of reservoir polaritons, which is consistent with the experimentally observed vortex [11]. The "observed" state is not a simple orbital angular momentum state, most of the structure come from the condensated eigenstate and the structure is further smeared by the non-condensed part so that the visibility is less than 1. We shall give the visibility of vortex core structure which is defined as

$$V = (N_{max} - N_{min})/(N_{max} + N_{min}), \tag{11}$$

where N_{max} and N_{min} are the maximal and minimal densities of the system, respectively. From $N_{max} = N(\rho \to \infty)$ and $N_{min} = N(\rho=0)$ for a vortex state, the visibility can be expressed by relaxation rates of the condensate and reservoir polaritons as $V = \alpha(\gamma_R - \gamma)/[\alpha(\gamma_R+\gamma)+2\gamma]$.

By solving Eq. (8) numerically, we can find the profile $f(\rho)$ using the shooting method [18,19] on the 4th order Runge–Kutta
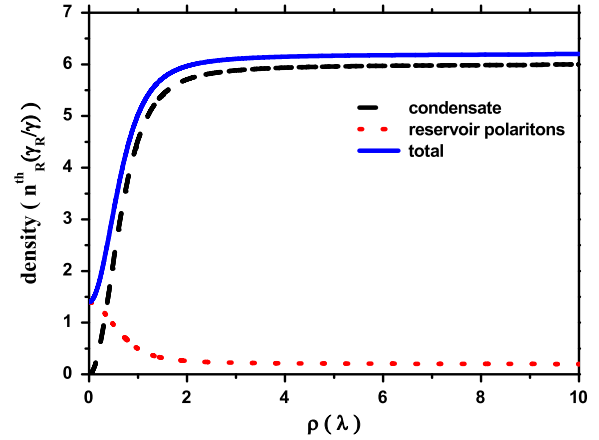

Fig. 1. (Color online) Spatial density profiles. Densities of the condensate and reservoir polaritons are shown by black dashed and red dotted lines, respectively. The blue solid line is the total density of the system.
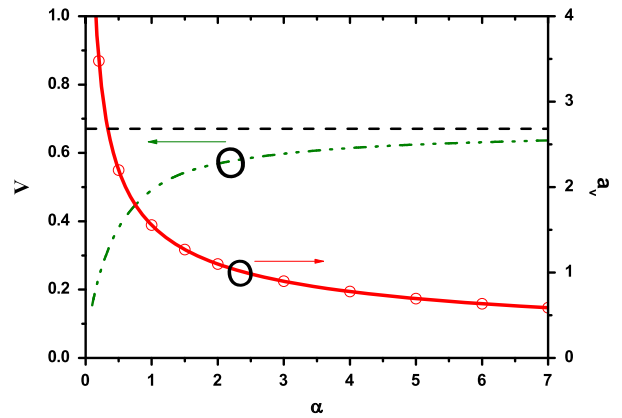

Fig. 2. (Color online) Core radii and visibility of vortices. The core radii (red circles) and visibility (green dash-dotted line) are plotted as a function of pumping power above the threshold. Red circles are core radii determined by using the half width at the half maximum of the total density, while the red solid line is the fitting curve of the core radius. The black dashed line indicates the maximal visibility of the vortex.

integration with boundary condition $f(\rho) \to 1$ as $\rho \to \infty$. To obtain numerical results we choose physical parameters used in Ref. [8]: $m\hbar^{-2} = 1.7$ meV^{-1} μm^{-2}, $\hbar\gamma = 1$ meV, $\hbar\gamma_R = 5$ meV, $\hbar g = 0.04$ meVμm^{-2}, and $\hbar n_R^{th} = 0.1$ me V μm^2. In Fig. 1, the density profiles of singly quantized ($\ell = 1$) vortex, reservoir, and their summation are shown in unit of $n_R^{th}(\gamma_R/\gamma)$ for $\alpha=6$. The vortex and reservoir densities are inversely related to each other. The condensate density decreases while the density of reservoir polaritons increases as $\rho \to 0$; and the total density at the center of a vortex is given by the density of reservoir polaritons. This is why the observed density inside the vortex core is not absolutely zero in the experiments. Moreover, the vortex radius a_V, which is defined from the half width at half maxima (HWHM) of the total density rather than the condensate density, is the actual core radius observed by experiments. For $\alpha=6$, the core radius $a_V \approx 0.6347\lambda$ is about 5.44 μm since the length unit $\lambda \approx 8.5749$ μm, and the visibility of vortex $V \approx 0.63$. The visibility and vortex radius for other pump strengths are shown in Fig. 2. The visibility and its vortex radius become more clear and smaller, respectively, as the pumping power increases. The numerical results (red circles) of the vortex radii can be fitted to a curve (solid red line) as $a_V = 1.5549\alpha^{-1/2}$. Therefore, $a_V \propto n_c^{-1/2}$ is confirmed from the relation of n_c and α, i.e., $n_c = (P_{th}/\gamma)\alpha$ [11,12]. As we raise the pumping power further, the visibility is saturated and approaches the maximal visibility $V_{max} = (\gamma_R - \gamma)/(\gamma_R + \gamma)$ having $V_{max} = 2/3$ for the case of $\gamma/\gamma_R = 0.2$. For the singly quantized vortices, the visibility of core structure increases with the pumping

power, however, the maximal visibility is limited by the decay rates of the condensate and reservoir polaritons.

The coreless vortex (nonzero density at center) we focus here is a consequence of the coupled equations between the polaritons from the reservoir and the condensate. If the condensated and non-condensated parts can be analogous to the two-component BECs with internal degrees of freedom like the spins, then the pseudo-spin representation can be implemented to find the skyrmion-like excitations. Then the coreless vortex we found here is "(baby)skyrmion-like", whereas, in atomic BECs, this kind of coreless vortex is observed in multi-component BECs and is often parametrized with different external field, rotation or trapping potential.

3. The stability and excitations of a vortex

After showing the steady-state properties of vortices, we investigate the excitations and stability of a singly quantized vortex. We consider small fluctuations $\delta\psi$ and δn acting on the steady state ψ_0 and n_0 of the system having a singly quantized vortex with an angular momentum characterized by quantum number ℓ. Because of the rotational invariance of the system, we assume

$$\delta\psi = u_q(\rho)e^{i(q+\ell)\theta}e^{-i\Omega\tau} + v_q^*(\rho)e^{-i(q-\ell)\theta}e^{i\Omega\tau} \quad (12)$$

and

$$\delta n = w_q(\rho)e^{iq\theta}e^{-i\Omega\tau} + w_q^*(\rho)e^{-iq\theta}e^{-i\Omega\tau} \quad (13)$$

where q and Ω are the quantum number (winding number) of the angular momentum of the excited state and the excitation frequency of the system, respectively. Then substituting $\psi = e^{-i\mu\tau}[\psi_0 + \delta\psi]$ and $n = n_0 + \delta n$ into Eqs. (3) and (4) and linearizing them around the steady state, we obtain three coupled Bogoliubov equations [20] that are used to study the excitations and stability of the system

$$-\Delta_+ u_q + (A(\rho)-\mu)u_q + B(\rho)v_q + C(\rho)w_q = \Omega u_q, \quad (14)$$

$$\Delta_- v_q - (A(\rho)-\mu)v_q - B(\rho)u_q - C^*(\rho)w_q = \Omega v_q, \quad (15)$$

$$-i\tilde{\gamma}_R[\alpha f(\rho)u_q + \alpha f(\rho)v_q + (1 + \alpha\beta f^2(\rho))w_q] = \Omega w_q, \quad (16)$$

where, the operators $\Delta_\pm = d^2/d\rho^2 + (1/\rho)d/d\rho - (q \pm \ell)^2/\rho^2$, together with the functions $A(\rho) = 2\alpha\sigma f^2(\rho) + (\sigma-1)[\kappa(\rho)/n_R^{th}]$, $B(\rho) = \alpha\sigma f^2(\rho)$, and $C(\rho) = [(i/2)\beta\tilde{\gamma} + (\sigma-1)]f(\rho)$ are separately defined and the dimensionless coefficient $\beta = R'(n_0)/R(n_0)$ is the change rate of the amplification on the reservoir density. For each pumping scheme, we get excitation frequency Ω as a function of q. There are many excitation states and we will be mostly interested in the branch with the lowest excitation frequency. The decay (Im(Ω) < 0) or growth (Im(Ω) > 0) behavior of the excitation mode indicates the steady state of the system is stable or unstable, respectively. Note that while there are solutions of three coupled Bogoliubov equations of the form (u_q, v_q, w_q), there should always have solutions of the form (v_q^*, u_q^*, w_q^*) with $\Omega_q \to -\Omega_{-q}^*$.

Discretization transforms the Bogoliubov equations into a matrix equation with eigenfrequencies and corresponding eigenfunctions solved under different pumping schemes, then we find the collective-excitation states and their excitation energies of the system. Here we only focus on the excitations of the singly quantized vortex ($\ell = 1$). The low-lying excitation modes with Re(Ω) ≥ 0 are shown in Fig. 3. The mode patterns are quite different for various pumping powers. Note that there exist dispersionless (Re(Ω) $= 0$) and strongly damped (Im(Ω) $= -5$) reservoir mode which is not shown here. This reservoir mode does not affect excitations of vortices much so that it will be neglected in our
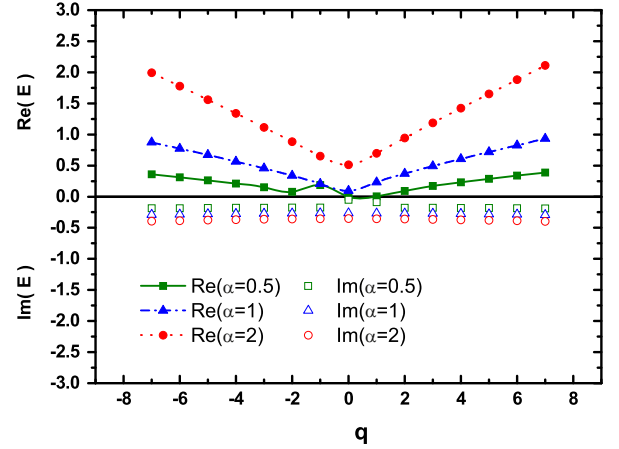

Fig. 3. (Color online) Excitation energies and decay rates of the excitations. Real parts (solid symbols) and imaginary parts (empty symbols) of excitation frequencies of singly quantized vortices are plotted as a function of winding numbers for $\alpha = 0.5$ (squares), 1 (triangles) and 2 (circles). The change rate, β, of the amplification on the reservoir density is equal to 1. Those lines connecting the solid symbols are shown to guide the eyes.

discussion of vortices. From Fig. 3, except for the cases of lower pump strength close to the threshold, excitation energies for a fixed pump strength increase with the winding number q. The excitation energies and decay rates of excitation modes for all q's also become larger as raising the pump strength. We find that finite excitation energies are needed in order to excite vortices in MPCs created by higher pumping powers. Once vortices appear spontaneously, they are very stable and not easily destroyed. From the experimental point view, MPCs created by higher pumping powers are easier to acquire enough angular momentum to form vortices [12]. There exists a wide range of pumping power above the threshold where Im(Ω) < 0, implying the singly quantized vortex mode is stable over a wide excitation window. This stability of vortices in MPCs indicates that vortices appear spontaneously without stirring or rotating MPCs that agrees with the experiment [12].

The MPCs vortices created by lower pumping power exhibit quite different behavior with the vortices created by high pumping power. The low-pump vortices exhibit zero excitation energies and a roton–maxon character for the small positive and negative q values, respectively, as long as α is less than 0.7. The asymmetric excitation spectra at lower pumping powers originate from the circulation quanta $\ell = 1$ existing in the operators $\Delta_\pm$ that the critical pumping power for asymmetric excitation spectra is to be determined by the relaxation rates of the condensate and reservoir polaritons. The effect of exciting vortices with no excess energy required shows that the low-pump vortices can transform spontaneously into excitation states with short lifetime [12]. Therefore, under low pumping power, MPCs are difficult to accommodate a vortex and can only be observed momentarily [12,21].

4. Conclusions

In conclusion, a numerical modeling using complex Gross–Pitaevskii equation is performed to understand the spontaneously formed vortices in homogeneous MPCs. We found that the densities of reservoir polaritons and condensed polaritons are locked together by the chemical potential. The reservoir density decreases as the condensate density increases and vice versa. Therefore, the center of the vortex core contains some background of reservoir polaritons, and the visibility of a vortex increases with the pumping power. Further increasing the pumping power, the

visibility would become saturated and approach a maximal visibility determined by the decay rates of the condensate and reservoir polaritons. Furthermore, the vortex radius is inversely proportional to the square root of the pumping power as well as the condensate density above the pumping threshold. The pumping power plays the role of quench rate in atomic BECs, acting together with the reservoir as the source of spontaneous vortex generation, which is a manifestation of the Kibble–Zurek mechanism. Excitations and the stability of a singly quantized vortex are also studied. We found a wide range of pumping power above the threshold having negative imaginary excitation frequencies for all winding numbers q's. Therefore, singly quantized vortices are stable and appear spontaneously without stirring or rotating MPCs. Excitation energies and decay rates of the excitation modes of vortices for all q's become larger with increased pumping power. The energies of vortices at high pumping power are finite and those at low pumping power are zero. Due to the existence of excitations without costing extra energy, vortices at low pumping power exhibit a short lifetime. Our observations in this paper are crucial and reachable for studying the vortex dynamics of polariton condensates in the future experiment.

Acknowledgments

References

[1] H. Deng, G. Weihs, C. Santori, J. Bloch, Y. Yamamoto, Science 298 (2002) 199.
[2] J. Kasprzak, M. Richard, S. Kundermann, A. Baas, P. Jeanbrun, J.M.J. Keeling, F.M. Marchetti, M.H. Szymánska, R. André, J.L. Staehli, V. Savona, P.B. Littlewood, B. Devaud, L.S. Dang, Nature (London) 443 (2006) 409.
[3] H. Deng, H. Haug, Y. Yamamoto, Rev. Mod. Phys. 82 (2010) 1489.
[4] S. Christopoulos, G. Baldassarri Höger von Högersthal, A.J.D. Grundy, P.G. Lagoudakis, A.V. Kavokin, J.J. Baumberg, G. Christmann, R. Butte´, E. Feltin, J.F. Carlin, N. Grandjean, Phys. Rev. Lett. 98 (2007) 126405.
[5] M. Wouters, I. Carusotto, Phys. Rev. Lett. 99 (2007) 140402.
[6] J. Keeling, N.G. Berloff, Phys. Rev. Lett. 100 (2008) 250401.
[7] M.O. Borgh, J. Keeling, N.G. Berloff, Phys. Rev. B 81 (2010) 235302.
[8] R. Balili, V. Hartwell, D. Snoke, L. Pfeiffer, K. West, Science 316 (2007) 1007–1010.
[9] K.G. Lagoudakis, M. Wouters, M. Richard, A. Baas, I. Carusotto, R. André, L.S. Dang, B. Deveaud-Plédran, Nature Phys. 4 (2008) 706.
[10] F.M. Marchetti, M.H. Szymańska, C. Tejedor, D.M. Whittaker, Phys. Rev. Lett. 105 (2010) 063902.
[11] D.N. Krizhanovskii, D.M. Whittaker, R.A. Bradley, K. Guda, D. Sarkar, D. Sanvitto, L. Vina, E. Cerda, P. Santos, K. Biermann, R. Hey, M.S. Skolnick, Phys. Rev. Lett. 104 (2010) 126402.
[12] D. Sanvitto, F.M. Marchetti, M.H. Szymanska, G. Tosi, M. Baudisch, F.P. Laussy, D.N. Krizhanovskii, M.S. Skolnick, L. Marrucci, A. Lemaitre, J. Bloch, C. Tejedor, L. Vina, Nature Phys. 6 (2010) 527.
[13] S. Utsunomiya, L. Tian, G. Roumpos, C.W. Lai, N. Kumada, T. Fujisawa, M. Kuwata-Gonokami, A. Löffler, S. Höfling, A. Forchel, Y. Yamamoto, Nature Phys. 4 (2008) 700.
[14] K.G. Lagoudakis, F. Manni, B. Pietka, M. Wouters, T.C.H. Liew, V. Savona, A.V. Kavokin, R. André, B. Deveaud-Plédran, Phys. Rev. Lett. 106 (2011) 115301.
[15] C.N. Weiler, T.W. Neely, D.R. Scherer, A.S. Bradley, M.J. Davis, B.P. Anderson, Nature 455 (2008) 07334.
[16] W.H. Zurek, Phys. Rep. 276 (1996) 177–221.
[17] M.H. Szymanska, J. Keeling, P.B. Littlewood, Phys. Rev. Lett. 96 (2006) 230602.
[18] M.A. Porras, A. Parola, D. Faccio, A. Dubietis, P.D. Trapani, Phys. Rev. Lett. 93 (2004) 153902.
[19] A. Alexandrescu, V.M. Pérez-García, Phys. Rev. A 73 (2006) 053610.
[20] N.N. Bogoliubov, J. Phys. (USSR) 11 (1947) 23.
[21] M. Wouters, V. Savona, Phys. Rev. B 81 (2010) 054508.